

MASS: a monitor of the vertical turbulence distribution

Victor Kornilov^a, Andrei Tokovinin^b, Olga Vozyakova^a, Andrei Zaitsev^a, Nicolai Shatsky^a,
Serguei Potanin^a, and Marc Sarazin^c

^aSternberg Astronomical Institute, Universitetsky prosp. 13, 119899 Moscow, Russia

^bCerro Tololo Inter-American Observatory, Casilla 603, La Serena, Chile

^cEuropean Southern Observatory, Karl-Schwarzschild Str. 2, 85748 Garching, Germany

ABSTRACT

The MASS (Multi-Aperture Scintillation Sensor) instrument consists of a 14-cm off-axis reflecting telescope and a detector unit which measures the scintillations of single stars in four concentric zones of the telescope pupil using photo-multipliers. Statistical analysis of these signals yields information of the vertical turbulence profile with a resolution of $\Delta h/h=0.5$. We describe the instrument and present the results of its first field tests, including comparisons with DIMM seeing monitor and generalized SCIDAR. MASS will be used to obtain the extensive statistics of turbulence profiles at potential sites of future giant telescopes, as needed to predict the quality of adaptive seeing compensation.

Keywords: turbulence profile, adaptive optics, site testing

1. INTRODUCTION

The performance of adaptive optics systems depends on the turbulence vertical profile $C_n^2(h)$ (hereafter TP) in many ways. The size of compensated field of view and the sky coverage with natural guide stars are constrained by the strength of high-altitude turbulent layers. The performance of laser guide stars depends on TP through cone effect and tilt anisoplanatism (isokinetic angle). The advanced turbulence-compensation techniques like multi-conjugate AO, ground layer compensation, etc. are also profile-dependent. Thus, monitoring of TP to support adaptive optics operation and to choose sites for future extremely large telescopes becomes a necessity.

Existing techniques for $C_n^2(h)$ measurements include a direct *in situ* balloon micro-thermal sounding and a remote optical sounding with double stars, known as SCIDAR. Both methods are not adapted for continuous profile monitoring. For this reason, no solid statistical database of $C_n^2(h)$ exists for any site.

Extraction of TP from the statistical analysis of scintillation of single stars is an attractive possibility for TP monitoring mentioned by many authors (e.g. Peskoff¹). The first single-star turbulence profiler was built by Ochs et al.² who called it *scintillometer*. Image of the telescope pupil was projected onto a checkerboard mask, the light fluxes transmitted and reflected by the mask were detected by two PMTs. Variance of the differential signal was related to the component of the spatial power spectrum of scintillations at the frequency of the checkerboard pattern. By scanning this frequency repeatedly over a certain range, Ochs et al. were able to measure part of the spatial power spectrum of scintillation and then reconstructed the TP with a vertical resolution of $\Delta h/h \sim 1$.

Multi-Aperture Scintillation Sensor (MASS) described below is a modern implementation of the same idea. Instead of a checkerboard mask, we use four concentric-ring apertures to probe the spatial structure of scintillation in the pupil plane of a small telescope. Fluxes passed by the apertures are detected by 4 photo-multipliers (PMTs) and analyzed statistically. This analysis is advanced in many respects compared to the simple first-order theory of scintillometer; however, the idea of *differential scintillation* employed in MASS can be traced back

Further author information: (Send correspondence to A.T.)

V.K., O.V., N.S.: E-mail victor, ovoz, kolja@sai.msu.ru

A.T.: E-mail: atokovinin@ctio.noao.edu

M.S.: E-mail: msarazin@eso.org

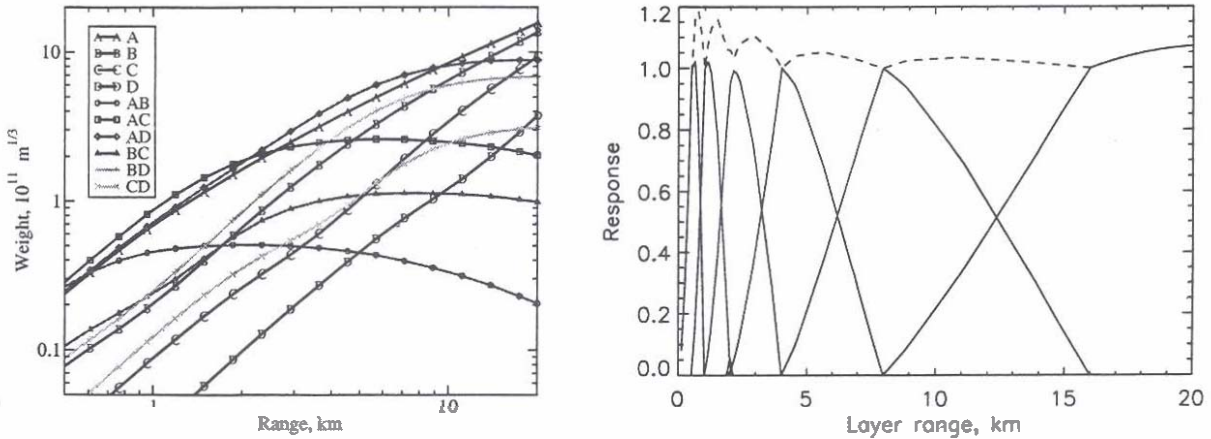


Figure 1. Left: weighting functions for the apertures and band-pass of MASS: normal scintillation indices for the apertures A, B, C, and D, and differential indices for aperture pairs. Right: Response of the fixed-layer restoration procedure to a single turbulent layer at variable distance. The response functions of the 6 pre-defined “slabs” are plotted in full lines, their sum – in dashed line.

to this early device. Our first results of turbulence characterization by single-star scintillation were published³ and enabled us to propose MASS at the IAU Workshop in Marrakesh.⁴

The principle of profile restoration in MASS will be mentioned only briefly in Sect. 2, because the main purpose of this article is to present the instrument (Sect. 3) and its first results (Sect. 4).

2. RESTORATION OF PROFILE FROM SCINTILLATION INDICES

Scintillation index is traditionally defined as a variance of light flux normalized by the square of the mean flux or, equivalently, as a variance of relative flux fluctuations.⁵ Four such *normal* indices are computed for the MASS apertures A, B, C, and D (labeled from inside out). Differential scintillation index for a pair of apertures was introduced in Refs. 6, 7 in a similar fashion, as a variance of the difference of relative flux fluctuations in both apertures. Six such indices are available in MASS.

For weak (non-saturated) scintillation, both normal and differential indices produced by a single turbulent layer are proportional to the intensity of a layer (integral of $C_n^2(h)$ measured in $m^{1/3}$) and depend on the distance (or range) to the layer, h . Normal indices always increase with the distance, whereas differential indices tend to constant values when the Fresnel radius $\sqrt{\lambda h}$ exceeds the diameter of the inner aperture. The ratio of scintillation index to layer intensity is called *weighting function*. Those functions were studied in Ref. 7 for monochromatic light, their generalization to polychromatic light is not difficult.⁸ A set of weighting functions for MASS is plotted in Fig. 1.

Any turbulence profile can be represented as a collection of independent layers. Ten scintillation indices measured by MASS are linear combinations of the layer intensities with the corresponding weighting functions. If we model the atmosphere as a collection of a small (less than 10) number of layers at pre-defined heights, this linear system of equations can be solved by the least squares method to find layer intensities from the measured indices. This is the principle of profile restoration.

The choice of a model (the number and altitudes of layers) is critical for a successful restoration. It is clear from Fig. 1 that relative “resolution” $\Delta h/h$ of a system of weighting functions is roughly constant, hence we used a logarithmic altitude grid with 6 fixed layers at 0.5, 1, 2, ..., 16 km. The restoration of TP is based on the least-squares with non-negativity constraint on the layer intensities. An alternative restoration procedure uses a model of three “floating” layers with arbitrary altitudes, also with 6 unknowns. Our experience shows that both fixed- and floating-layer models produce adequate fits to the observed scintillation indices and hence extract all the information on TP contained in the data.

The detailed description of the data processing, from raw photon counts to profile restoration, will be published separately. Our numerical simulations have shown that the restoration process is quite stable. The altitude resolution of $\Delta h/h \sim 0.5$ is indeed achievable: the "response function" of a given layer is of triangular shape, with a maximum at the nominal layer altitude and falling to zero on both sides at the adjacent layers (Fig. 1). The sum of all response functions is practically constant at altitudes above 0.5 km. For this reason the integral of turbulence (hence seeing) is determined particularly well, with a relative error of less than 5%. For a fixed-layer model, the errors of layer intensities depend on the altitude (smaller errors for higher layers) and on the profile itself; for strong layers they are of the order of 10% or less.

3. THE MASS INSTRUMENT

3.1. Optical layout

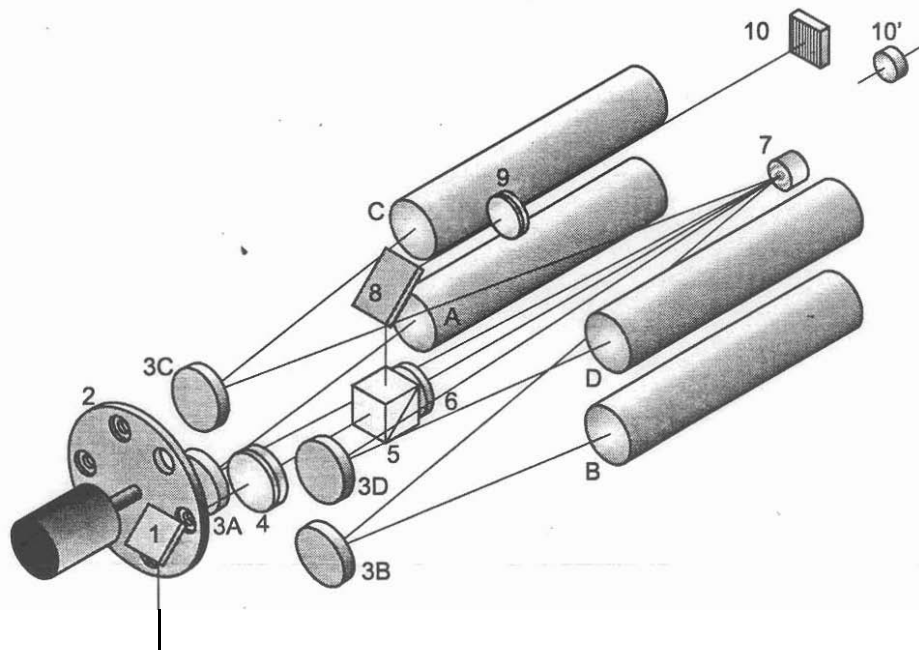


Figure 2. Optical layout of the MASS detector module (see text).

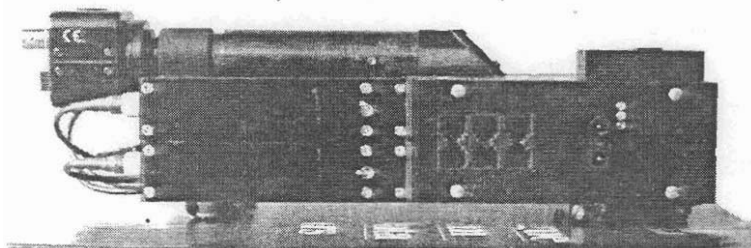


Figure 3. Photograph of the detector box. The buttons for manual control and the mounting flange are seen on the right, the two PMT modules and the viewer with guiding TV camera – on the left, the connectors to the RS-485 line – at the center. The length of the detector box is 21 cm.

The nominal diameters of the four concentric apertures are chosen as 2, 3.7, 7.0, 13 cm. Thus, MASS needs a feeding optics with a clear (unobstructed) aperture of at least 13 cm. An off-axis portion of a larger telescope pupil with central obstruction can be used, for example. For stand-alone turbulence monitoring, we built an off-axis reflecting telescope with a 14 cm elliptic primary and a spherical secondary. Other solutions, e.g. refractive optics, are also possible.

The light of a bright star collected by the feeding telescope enters the detector box (Fig. 2). Upon reflection from the folding mirror 1, it passes through the focal aperture mounted on the disk 2 controlled by the stepper

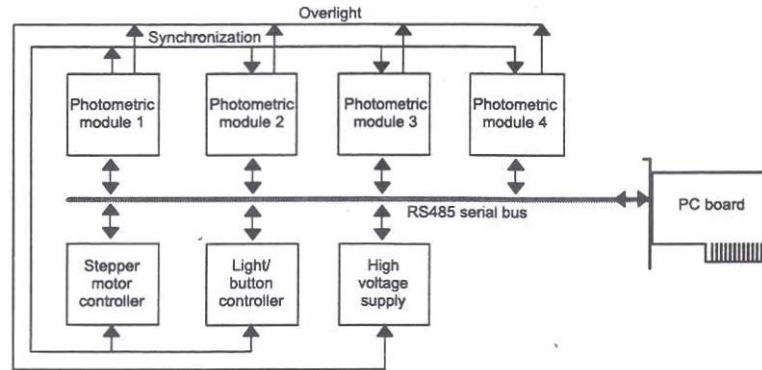


Figure 4. Block diagram of the MASS electronics.

motor. The Fabry lens 4 forms an image of the telescope pupil on the “segmentator” 7 with a de-magnification factor around 20. The segmentator consists of four concentric mirrors with different tilts, each mirror reflecting the beam at a certain angle. The diameter of the inner mirror is 1 mm, the diameter of the outer mirror is 6.5 mm (2 cm and 13 cm, respectively, as projected onto the telescope pupil). The four reflected beams fall on the spherical mirrors 3A-3D which re-image pupil at the photo-cathodes of the PMTs A, B, C, and D.

The dichroic beam-splitter 5 reflects the light with wavelengths long-wards of 600 nm to the viewer which consists of the folding mirror 8, the lens 9 and the eyepiece 10, which can be replaced by a small TV camera 10. Spectral filtering of the detected light is provided by the glass filter 6 glued to the beam-splitter.

The segmentator is a non-standard, custom-made optical element. First, four closely matched cylinders were machined from stainless steel and assembled together. Then the working surface was ground and polished at an angle with the cylinder’s axis. The surface is made slightly concave to avoid the divergence of the reflected beams. After aluminization, the cylinders were turned around their common axis and the segmentator was re-assembled in its final configuration.

3.2. Detectors

In principle, a CCD detector can be placed in the exit pupil plane instead of the segmentator. It is clear that a very fast CCD (1000 frames/s) with a low readout noise (less than 5 electrons) is needed here. Such a solution would have a significant advantage — apertures of different size and shape could be defined in the software rather than in the hardware. But in order to reach an accuracy of indices of about 1% with stars of magnitude 2, the value of the readout noise (which degrades normal photon statistics) must be also known within 1%.

To avoid such technical challenge, bi-alkali photo-multipliers R-647P from Hamamatsu were selected as light detectors. The pulse amplifiers and discriminators have a dead time of 17 ns, as inferred from the dependence of the flux variance on the counting rate.⁹ The flux variance closely follows the Poisson law. We measure the *non-Poisson parameter* $p = \overline{\Delta N^2} / \bar{N}$ of 1.00 - 1.05, typically. The photon counts are sampled with a micro-exposure time of 1 ms. A star of B=2 magnitude gives a counting rate of 33 pulses per ms in the smallest 2-cm aperture, A. To account correctly for the photon statistics, the value of p must be known with an accuracy of 0.01 or better.

The spectral sensitivity of PMTs and the glass filter define the spectral response of MASS. The final response curve also depends on the spectral energy distribution of the observed stars. The photometric passband is located between the standard photometric V and B pass-bands, its effective wavelength is about 470 nm, the effective width is about 90 nm for stars of spectral type A0.

3.3. Electronics

The MASS electronics (Fig. 4) consists of 7 separate independent modules. The architecture of all modules is similar. The core of any module is an Atmel AVR micro-controller AT90S2313. A great merit of these controllers is the possibility of their re-programming in field conditions.

The four photometric modules include both PMTs and the associated electronics which consists of a very fast amplifier-discriminator, a counter linked to micro-controller and an interface circuit. The main function of those modules is to count the PMT pulses during series of microexposures and to transmit these data to the host computer. The commands from the host computer permit to set the level of pulse discrimination, to run series of micro-exposures, to set the exposure time (or to slave exposures to the external synchro signal), to set the length of data series, etc.

The stepper motor module consists of a stepper motor, a motor driver, null-point and entrance-shutter sensors. The device provides a microstepping mode with 3200 steps per revolution. The module enables fast and accurate setting of apertures on the optical axis and scanning of the stellar image by moving apertures. To diminish the switching time from one disk position to another, the motor rotates with programmed acceleration and deceleration. In the scanning mode, the motor speed is constant and synchronized with an external clock.

The light and buttons controller regulates the current through the two LEDs: the red LED illuminating apertures and the green control LED used to check the PMTs and to measure their parameters. This module also polls the 3 buttons for manual control of the MASS which are used during adjustments or tests.

The high voltage module produces a controlled voltage from 0 to 1250 V for PMTs. In an emergency situation of excessive PMT illumination a special signal from the photometric modules turns off the high voltage immediately, by-passing any computer control. Additional functions provided by this module are the monitoring of the MASS internal temperature and of the RS-485 line status.

All modules are connected to the host computer via a half-duplex RS-485 line in a multi-drop configuration. Two additional internal lines are used for to transmit the synchronization signal common to all modules of the modules and for the fast hardware protection of PMTs against over-light. MASS operation needs a data transmission rate as fast as 8 Kb/sec (or 110 Kbit/sec). The chosen micro-controller clock frequency provides the exchange rate of up to 460.2 Kbit/sec which is adequate for our purpose. To support such data exchange, a commercially available high-speed RS-485 interface board is used in the PC computer.

A special communication protocol ensures an effective and faultless data exchange in binary format, merged in packets of 1 to 31 byte length. All MASS modules work as passive devices — they can transmit data only in response to a request from the host computer. The photometric modules can also work as active devices, i.e. they can initiate the packet transmission when a next data block is ready. This leads to a more efficient data acquisition compared to polling. A special driver was developed to service this protocol. Since MASS operation requires from the host computer a guaranteed reception of a 19-byte packet each 2 ms, Real-Time Linux¹⁰ was chosen as operating system. We succeed in reducing the data loss probability to below 10^{-5} .

3.4. Software

The MASS control software, *Turbina*, is coded in C++ language and operates under RT Linux in X-11 graphic environment. *Turbina* opens two main windows — one for graphic user interface with menu-driven commands, the second one — for graphical output of selected parameters and turbulence profiles during observations. All operational and instrumental parameters are kept in editable configuration files and can be changed during observations.

A number of tests can be executed (either manually or automatically) before observations. They include the exchange test (verification of electronics and its interface to PC), the detector test (measurement of the fluxes from control light source and of non-Poisson parameter), and the statistical test when the light of the control source is modulated and the scintillation indices are computed as in real observations. The background (sky light in the aperture and dark counts of PMTs) must be measured before the observations and when conditions change (moon-rise etc.). Typically, the background is less than 1% of stellar flux in all channels. A suitable star can be selected from the on-line catalog which shows the objects sorted on zenith distance, magnitude, etc. The color of the selected star is taken into account in choosing the appropriate weighting function (a set of such functions for all color classes and for the specific instrument parameters is pre-computed by *Turbina*). The zenith distance of a star, z , must be taken into account in the profile restoration: the distance to the layers is increased by $\sec z$ times compared to layer altitudes and the observed layer strengths are increased by $\sec z$ times as well.

A normal observation consists of data accumulation during 1 minute. The scintillation indices are computed for each 1-s segment of data and then averaged. This permits to estimate the real errors of average indices from the scatter of their 1-s values. The average indices are used immediately for profile restoration by two methods (fixed and floating layers). Additionally, the moments of the turbulence profile (as needed for seeing and isoplanatic angle derivation) are computed directly as linear combinations of 1-s indices and then averaged over 1 min.

The position of the star in the field can be determined by scanning with triangular aperture. This is useful for *a posteriori* checks of data quality and for automatic guiding.

Sequences of observations that do not require manual intervention are programmed and executed as *scenarios*. A typical scenario can include a background estimate, then centering/guiding and profile measurement every minute during 1 or 2 hours. Additional operations like tests or shutdown may be included in the scenario as well. In the near future when telescope pointing is automated, the MASS instrument will be operated in robotic mode.

4. FIRST RESULTS

The first MASS instrument started operation at Cerro Tololo in Chile in March 2002. The second instrument belonging to ESO was commissioned in May 2002. Some 50 nights of data are accumulated by now for Cerro Tololo. Sample results and tests are presented below.

4.1. Cross-check with DIMM

Integral of turbulence profile measured by MASS gives an estimate of “free-atmosphere seeing” ϵ_f , i.e. the seeing that one would obtain without lowest layers. The borderline between the ground layer and the free atmosphere is a matter of convention; here we include in the free atmosphere all layers from 0.5 km up (the dashed line in Fig. 1-right). In fact, MASS response falls smoothly below 0.5 km, so a turbulence at, say, 0.3 km is also sensed with a reduced weight.

Whenever layers above 1 km dominate the overall integral of $C_n^2(h)$, the free-atmosphere seeing ϵ_f approaches the total seeing ϵ as measured by a differential image motion monitor (DIMM). In other circumstances the condition $\epsilon_f < \epsilon$ must hold. This is indeed the case, as shown in Fig. 5b for one night: after 8:30 UT both DIMM and MASS measured the same seeing. The conditions when $\epsilon_f \approx \epsilon$ were observed repeatedly at Cerro Tololo during the first months of MASS operation. Several episodes of strong turbulence with a typical duration of ~ 0.5 hour often occur during a night, explaining the “spikes” of degraded seeing. Strong turbulence may be low (0.5-1 km) or high (4-8 km), but whenever it dominates the total seeing there is always a match between MASS and DIMM.

The good agreement between MASS and DIMM, the two instruments based on different principles, is a confirmation of the theory of optical propagation used to interpret scintillation and image motion in terms of seeing. At the same time it strengthens the confidence in the absolute calibration of MASS.

4.2. The quality of profile restoration

The relative errors of the scintillation indices averaged over 1 minute are, typically, between 1.5% and 2%, independently of aperture and stellar flux. This “noise” comes from the statistical nature of the scintillation signal itself, this is why the signal-to-noise ratio remains so remarkably constant. If each 1 ms sample of light intensity were independent of other samples, we would expect to measure scintillation index with a relative error of $(60000)^{-1/2} = 0.4\%$. In fact 1 ms samples are strongly correlated and, moreover, part of the indices’ scatter comes from the fast variations of $C_n^2(h)$. The relative errors of the differential indices are comparable to those of the normal indices, except for the AB aperture pair where the error increases to 3% - 4%. This pair has the smallest index and is influenced by the photon noise.

The very first impression from the turbulence profiles measured with MASS was their good repeatability in sequential 1-minute intervals. The overall quality of restoration is assessed by the χ^2 parameter – the sum of the squares of residuals between measured and modeled scintillation indices normalized by the variances of

the measured indices. Most of the time we obtain $\chi^2 < 10$. In Fig. 5d the detailed plot of relative differences between measured and modeled scintillation indices is given to show that the model always fits the data to better than 5%, despite significant variations of the TP structure.

The two restoration methods (with fixed and floating layers) give complementary view of the TP structure. Whenever a strong layer is present, it is well-localized by the “floating” method: successive measurements show consistent results. On the other hand, thick, distributed turbulence can be identified by random altitudes obtained from one minute to the next. The integrals of TP obtained by both methods agree with each other (and with the direct estimate of zeroth moment) very well, with a difference in corresponding seeing of less than $0.02''$.

A constant signal-to-noise ratio means that the sensitivity of MASS improves as the turbulence becomes weaker. A calm upper atmosphere produces a typical seeing of $\epsilon_f \approx 0.2''$ (between 2h and 3h in Fig. 5). In

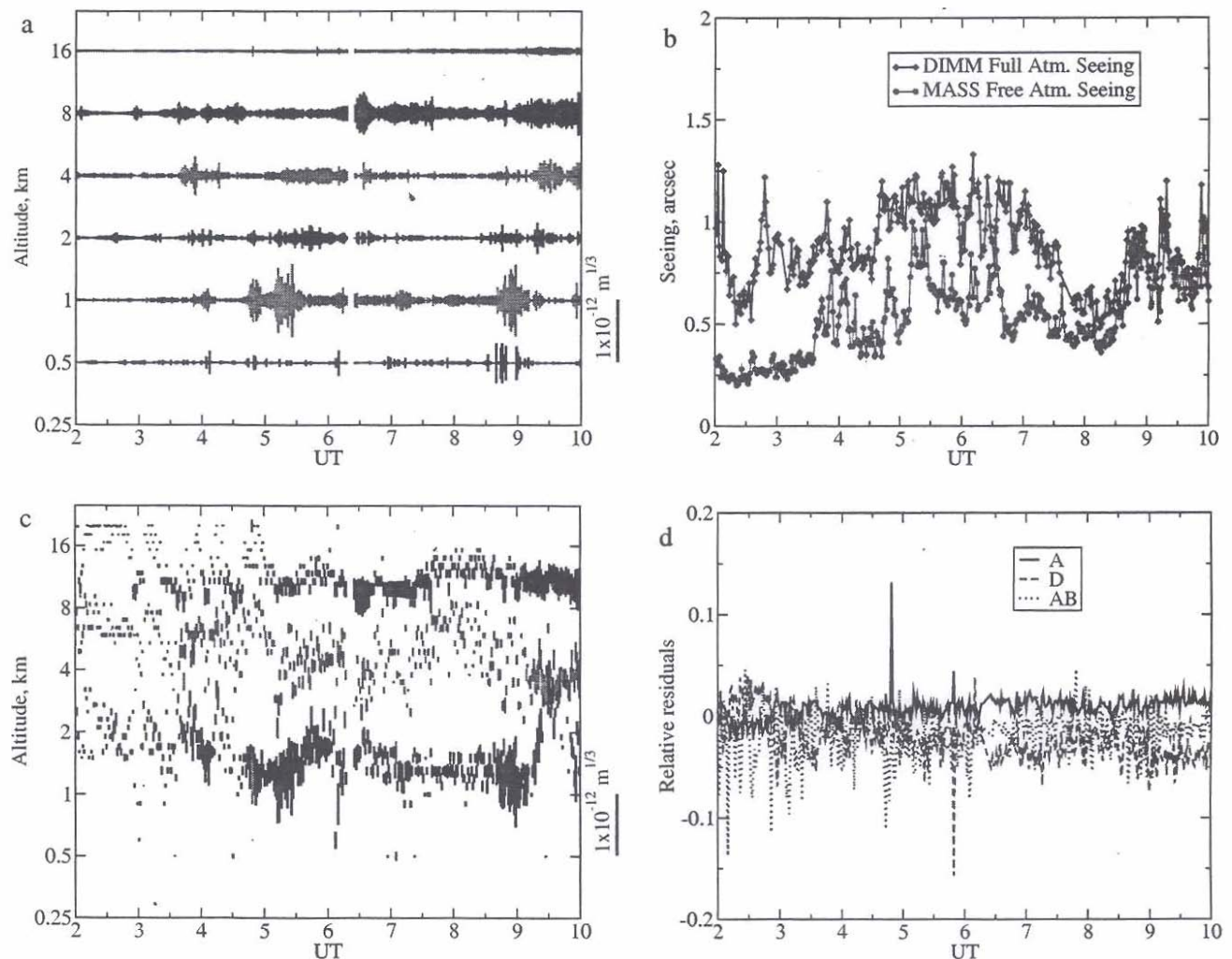


Figure 5. Sample results of MASS at Cerro Tololo for the night of July 14-15, 2002, as a function of the universal time UT in hours. **a:** Turbulence profiles restored with fixed layers, the bar lengths are proportional to the intensity of each layer with a scale indicated to the right. **b:** Comparison of the total atmospheric seeing ϵ as measured by a DIMM monitor (upper curve) and the free-atmosphere seeing ϵ_f as deduced from the MASS profiles (lower curve). **c:** Turbulence profiles restored with a model of 3 floating layers. **d:** Relative difference between the measured scintillation indices (normal in apertures A and D and the differential for the pair AB) and the indices computed from a fixed-layer profile restoration.

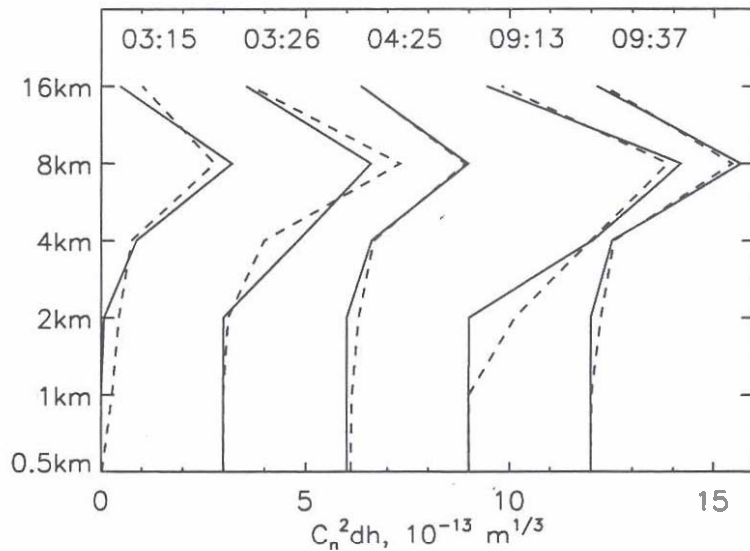


Figure 6. The low-resolution turbulence profiles measured simultaneously by MASS (full lines) and SCIDAR (dashed lines) at La Silla on July 10-11, 2002. The profiles were shifted horizontally by 3 units for clarity, numbers above indicate the UT. All SCIDAR profiles except the one at 04:25 UT were obtained in non-generalized mode.

these conditions MASS still gives well-reproducible profiles.

4.3. Comparison with SCIDAR

A campaign of comparison between MASS and SCIDAR was started in July 2002 at the La Silla ESO observatory. This campaign is not yet finished, only some first preliminary results are given here. The SCIDAR is built by a group at the Imperial College, London, it is described by Klückers et al.¹¹ As mentioned in the publication, the integrals of TPs given by this SCIDAR are unrealistically low. For the sake of comparison, we re-normalized the SCIDAR TPs to match the integral strength of MASS TPs at altitudes above 4 km (at lower altitudes, SCIDAR in non-generalized mode is not reliable) and convolved them with the triangular response functions of MASS. In Fig. 6 the comparison of few profiles reduced so far is presented. The SCIDAR TPs were obtained with only 5.3 s integration time and refer to a different direction on the sky respective to MASS. Given the high spatial and temporal variability of turbulence, the agreement between the two instruments is as good as it can be: both identify a strong turbulent layer around 8 km with little turbulence below and above.

4.4. Generalized mode

Originally we planned to measure the lowest (ground) layer in the so-called *generalized* mode. In this mode, a small positive lens is placed in the focal plane to introduce an additional virtual propagation, like in generalized SCIDAR or in a curvature wave-front sensor. For a feeding telescope with a large aperture, the effect would correspond to a shift of all weighting functions to the left, giving MASS some sensitivity to the ground-layer turbulence. However, a feeding telescope with a small 14-cm aperture in generalized mode has two undesirable effects. The diffraction on the entrance aperture causes significant light modulation in the plane of segmentator, even without any turbulence. We have shown by simulation that the differential and normal scintillation indices are not affected by diffraction as long as the shift is less than 0.5 km. The second effect is a displacement of the defocused pupil over the segmentator when a star moves in the focal plane. Again, the simulations indicate that for our instrumental configuration the rms image jitter up to 4'' is tolerable.

The actual experiments have shown that the seeing measured by MASS in generalized mode was always larger than the atmospheric seeing measured by DIMM by a factor that varied between 1.1 and 2. We attribute this difference to the turbulence in the open tube of the feeding telescope and, possibly, to the effects of pointing errors and jitter. Given the strict pointing requirements, we believe that the generalized mode would be anyway impractical for a small and robust turbulence monitor.

5. CONCLUSIONS AND PLANS

The first results obtained with MASS are encouraging. We have demonstrated that it is capable to resolve the turbulence profile into 6 layers and to measure the strength of each layer with sufficient accuracy. The instrument is cheap and simple, well suited for systematic monitoring of TP. We have already started to study the statistics of turbulence over Cerro Tololo.

The next step would be to combine MASS and DIMM in one instrument that would be capable to measure both integrated turbulence intensity (seeing) and its vertical distribution (profile). The apertures of MASS will become smaller to fit into the 8 cm clear space in the pupil of cheap amateur telescopes that are typically used to feed DIMMs. Part of the pupil unused by the DIMM will feed MASS. On the other hand, the DIMM will conveniently provide pointing and guiding. When a sufficiently stiff and reliable telescope mount under computer control is available, we shall develop a completely robotic monitor of atmospheric turbulence.

ACKNOWLEDGMENTS

Since 1997, the head of the ESO AO team, Norbert Hubin, gave us a strong encouragement to develop single-star turbulence monitor for the needs of AO and consistently supported this effort. We are grateful to the personnel of Cerro Tololo and La Silla observatories for the help they provided in the initial installation of the new instruments at the respective sites. The MASS data at Cerro Tololo are being acquired by Sylvain Baumont and Joselino Vasquez. The efforts of Chris Dainty, Chris Walker, and David Lara-Saucedo from the Applied Optics Group of the Blackett Laboratory of IC, London, to bring SCIDAR and to teach us how to use it are deeply appreciated.

REFERENCES

1. A. Peskoff, "Theory of remote sensing of clear-air turbulence", *J. Opt. Soc. Am.*, **58**, pp. 1032-1040, 1968.
2. G.R. Ochs, Ting-i Wang, R.S. Lawrence, and S.F. Clifford, "Refractive-turbulence profiles measured by one-dimensional spatial filtering of scintillations", *Appl. Opt.*, **15**, pp. 2504-2510, 1976.
3. V.G. Kornilov and A.A. Tokovinin, "Measurement of the turbulence in the free atmosphere above Maidanak", *Astronomy Reports*, **45**, pp. 395-408, 2001.
4. A. Tokovinin and V. Kornilov, "Measuring turbulence profile from scintillations of single stars", in: *Astronomical Site Evaluation in the visible and Radio Range*, Z. Benkhaldoun, C. Muñoz-Tuñon, and J. Vernin, eds., ASP Conf. Ser., 2001 (Marrakesh, November 13-17, 2000)
5. F. Roddier, "The effects of atmospheric turbulence in optical astronomy", in: *Progress in Optics*, E. Wolf, ed., North-Holland, **19**, pp. 281-376, 1981.
6. A.A. Tokovinin, "A new method to measure the atmospheric seeing", *Astronomy Letters*, **24**, pp. 662-664, 1998.
7. A.A. Tokovinin, "Measurement of seeing and atmospheric time constant by differential scintillations", *Appl. Opt.*, **41**, pp. 957-964, 2002.
8. A.A. Tokovinin, "Polychromatic scintillation", 2002, in preparation.
9. V.G. Kornilov and T.M. Pogrosheva, "Non-traditional method for the investigation of photodetector receiver nonlinearity", *Astron. Zhourn*, **66**, pp. 424-425, 1989.
10. M. Barabanov and V. Yodaiken, "Real-time linux", *Linux journal*, February 1997.
11. V.A. Kfückers, N.J. Wooder, T.W. Nicholls, M.J. Adcock, I. Munro, and J.C. Dainty, "Profiling of atmospheric turbulence strength and velocity using a generalised SCIDAR technique", *Astron. Astrophys. Suppl. Ser.*, **130**, pp. 141-155, 1998.